The First-Order Spin-Wave Instability Threshold in Saturated and Partially Magnetized Spheres, Rods, and Disks of Polycrystalline Yttrium Iron Garnet at 9.1 GHz

CARL E. PATTON AND JEROME J. GREEN, SENIOR MEMBER, IEEE

Abstract—The first-order spin-wave instability threshold has been measured at 9.1 GHz for polycrystalline yttrium iron garnet as a function of sample shape, sample orientation, pump configuration, and magnetization stake. Spheres, rods, and thin disks were used. The results for saturated samples show that sample shape has a strong influence on the threshold. The data are in good argeement with theory, except for the thin disk samples. The disk data are affected strongly by annealing and the threshold field dependence on static field is modified by inhomogeneous demagnetizing fields. Results for partially magnetized samples indicate that the theory for saturated samples is directly applicable to partially magnetized systems if demagnetizing factors appropriate to the domain shape and not sample shape are used. In the limit of zero external field, the threshold for thin disks with the microwave field in the disk plane is equal to the perpendicular pump threshold for axially magnetized rods. This result indicates that the thin disks demagnetize by the formation of rod-shaped domains oriented normal to the disk. The disk results for pumping with the microwave field normal to the disk are also consistent with this qualitative domain model. Domain shape appears to play essentially the same role in determining thresholds for partially magnetized systems that sample shape does for saturated systems.

I. Introduction

MOST investigations of the first-order spin-wave instability threshold in ferrites and garnets have utilized spherical samples magnetized to saturation. Materials incorporated in devices are usually not spherical in shape and are often used in a partially magnetized state. The high-power limits on the device may be quite different from predictions based on threshold data for saturated spherical samples. The influence of sample shape and magnetization state on the threshold must be taken into account. In order to characterize these influences, threshold data have been obtained for parallel and perpendicular pumping at 9.1 GHz in spheres, rods, and thin disks of polycrystalline YIG for static external fields between zero and 2200 Oe. The results above saturation were compared with theoretical thresholds obtained from a recent extension [1] of the first-order spin-wave instability theory originally developed by Suhl [2] and Schlömann [3]. The data are in good agreement with theory. The results for partially magnetized or demagnetized samples were related to the data for saturated samples on the basis of domain structure considerations. The theory for saturated systems appears to be directly applicable to partially magnetized samples if demagnetizing factors appropriate to the domain shape, not sample shape, are used.

Manuscript received March 17, 1969; revised May 19, 1969. Paper 28.9, presented at the 1969 INTERMAG Conference, Amsterdam, The Netherlands, April 15–18. This work was supported by the Advanced Projects Agency of the Department of Defense and was monitored by the Rome Air Development Center under contract F30602-68-C-005.

The authors are with the Research Division, Raytheon Company, Waltham, Mass.

II. Experimental Procedure

Although experimental techniques for determining the instability threshold h_{crit} in ferromagnetic insulators are well known [4], two aspects of the present technique depart significantly from previous procedures. These are 1) automation of the instrumentation for threshold determination and 2) sample alignment procedures.

The threshold h_{crit} can be determined by measuring the reflection coefficient Γ of an undercoupled microwave cavity as a function of the microwave field amplitude h. For $h < h_{crit}$ (below threshold) Γ is independent of h. Above threshold, Γ increases sharply with h. The standard experimental procedure is to measure Γ for a cavity containing the sample as a function of h, point by point, and determine h_{crit} as the break in the curve. A semiautomatic instrumentation system has been developed which simplifies the above procedure considerably. The system allows curves of log Γ to be plotted automatically as a function of h^2. Values of h_{crit} can be easily and rapidly determined from the recorder plots. The instrumentation is designed around a standard reflection cavity microwave spectrometer [4]. A 2J51 magnetron source operated in a pulsed mode feeds 4-μs pulses at a 60-Hz repetition rate to a TE_{102} 9.1-GHz rectangular cavity. Sample and hold circuits are used to extract dc voltages which are proportional to the pulse amplitudes for the pulses incident on and reflected from the cavity. Crystal tracking problems are eliminated by using a single detector to sample the incident and reflected pulses on alternate cycles through a SPDT microwave switch. The dc voltages drive logarithmic converters which feed the two inputs of a differential amplifier. The amplifier output drives the y axis of a pen recorder and is proportional to log Γ. The x axis is driven by the recorder output of a microwave power meter which measures the incident power. A more detailed description of the automatic system will be published elsewhere.

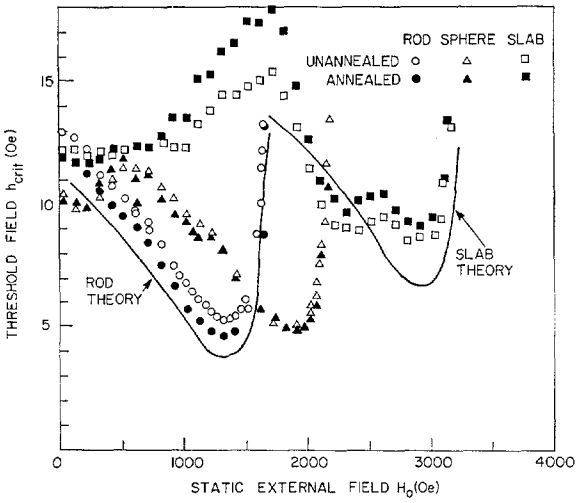

Fig. 1. Threshold field h_{crit} as a function of static external field H_0 for axially magnetized 40-mil-diameter rods, 1-mm-diameter spheres, and normally magnetized 10-mil-thick 1-cm-diameter disks, before and after 1-hour anneal at 1000°C. Solid lines were obtained from theory as explained in text.

Alignment was extremely critical, particularly for disk shaped samples. For a normally magnetized 20-mil-thick 1-cm-diameter YIG disk, misalignment of a few degrees results in a substantial change in both the value of h_{crit} and the shape of the so-called butterfly curve (h_{crit} versus static field). In order to ensure accurate sample alignment, the cavity was mounted on a circular plate which could be tilted about two perpendicular axes in the plane of the plate. Alignment was accomplished at low power with a CW klystron source. Accurate alignment to $\pm 0.1°$ could be accomplished by minimizing or maximizing the reflected power from the cavity (depending on the sample shape and orientation) with the sample biased on the low-field side of resonance.

III. Results and Discussion

A. *Sample Shape and the Perpendicular Pump Threshold*

Large changes in sample shape have a profound influence on h_{crit}. In Fig. 1 the threshold field h_{crit} is shown as a function of static external field H_0 for perpendicular pumping in 1-mm-diameter spheres, axially magnetized 40-mil-diameter rods, and normally magnetized 1-cm-diameter 10-mil-thick disks of polycrystalline YIG. Data are shown both before and after a one-hour anneal at 1000°C. Except for the shift to higher static field and the small decrease in h_{crit} below $H_0 = 600$ Oe, the experimental results for the sphere are similar to those for the axially magnetized rod. The data for the 10-mil-thick normally magnetized disk, however, are quite different. In general, h_{crit} is significantly larger for the disk than for either the sphere or rod. The disk threshold increases from 12 Oe at $H_0 = 0$ to 18 Oe at 1700 Oe, exhibits two local minima at 2300 and 2900 Oe, and increases sharply at higher field.

It is well known that the internal magnetic fields, both microwave and static, are influenced by geometry and that the action of these fields on the local magnetization determine, in part, the high-power properties of the sample. These points can be demonstrated more quantitatively by considering theoretical curves of h_{crit} versus static field H_0 for the sample shapes of interest. Theoretical values were obtained as follows: 1) the data on spherical samples were used to calculate the spin-wave linewidth ΔH_k as a function of wave vector $\boldsymbol{k}$ using the theory developed in [1]; the ΔH_k determined in this way was incorporated into the theory for the rod and disk shapes and h_{crit} versus H_0 curves were obtained for these geometries. A brief discussion of the ΔH_k results is given in the Appendix. The rods and disks were approximated by ellipsoids of revolution with axes corresponding to the appropriate sample dimensions. Theoretical curves are indicated by the solid lines in Fig. 1. No curve is shown for the sphere because those data were used to evaluate ΔH_k. The rod data are in good agreement with the calculated curve which was obtained with no adjustable parameters. The agreement for the normally magnetized disk is poor. The theoretical minimum is somewhat lower than indicated by the data and the calculated curve does not exhibit the double minimum.

The theoretical curves are similar in shape but shifted upward and outward with increasing axial demagnetizing factor N_z. The outward shift (to higher H_0) is due to the increase in the static internal demagnetizing field with N_z. The shift toward higher h_{crit} values is due to a decrease in the efficiency with which the microwave field pumps the uniform precession amplitude α_0. For samples with rotational symmetry about the static field direction, the main contribution to α_0 is due to the Larmor component of the pump field and is given by

$$\alpha_0 = [h \exp(i\omega t)]/2(\omega_0 - \omega) \tag{1}$$

where

$$\omega_0 = \gamma[H_0 + (N_t - N_z)4\pi M] \tag{2}$$

is the uniform precession frequency. In the above equations, N_t is the transverse demagnetizing factor ($N_z + 2N_t = 1$), $4\pi M$ is the saturation induction, and ω is the angular excitation frequency. For a constant microwave field amplitude and H_0 corresponding to the butterfly curve minimum, $|\alpha_0|$ decreases with increasing N_z. Since the coupling between the microwave field at ω and the spin-wave modes at $\omega/2$ which leads to the first-order instability is proportional to $|\alpha_0|$, a reduced $|\alpha_0|$ results in an increased threshold. The minimum threshold therefore increases with N_z. The differences between the disk data and the theory near the minimum are probably associated with the rather inhomogeneous demagnetizing fields in the thin disk. At the center of the disk this field is approximately $4\pi M$, while near the edge it is only half this value. For YIG the difference is about 800 gauss, which is on the order of the separation of the two minima for the disk data in Fig. 1.

The relatively short one-hour anneal at 1000°C had a negligible effect on the sphere data, decreased h_{crit} by about one Oe for the rod, and increased h_{crit} by as much

TABLE I
SUMMARY OF EXPERIMENTAL RESULTS FOR PARALLEL AND PERPENDICULAR PUMPING IN THIN 1-CM-DIAMETER DISKS OF POLYCRYSTALLINE YTG AT 9.1 GHz

Configuration	Nature of Thickness Dependence	Minimum h_{crit} Position	Nature of High Field Increase	Change in h_{crit} upon Demagnetization
Parallel pump ($\perp,\perp,\parallel$)	Large decrease	2500 Oe	Sharp increase	No change
Parallel pump ($\parallel,\parallel,\parallel$)	Small decrease	1100 Oe	Moderate increase	Large increase
Perpendicular ($\perp,\parallel,\perp$)	Moderate decrease	2500 Oe (broad)	Sharp increase	No change
Perpendicular ($\parallel,\parallel,\perp$)	Negligible	1500 Oe (broad)	Moderate increase	No change
Perpendicular ($\parallel,\perp,\perp$)	Large decrease	1400 Oe	Moderate increase	Large decrease

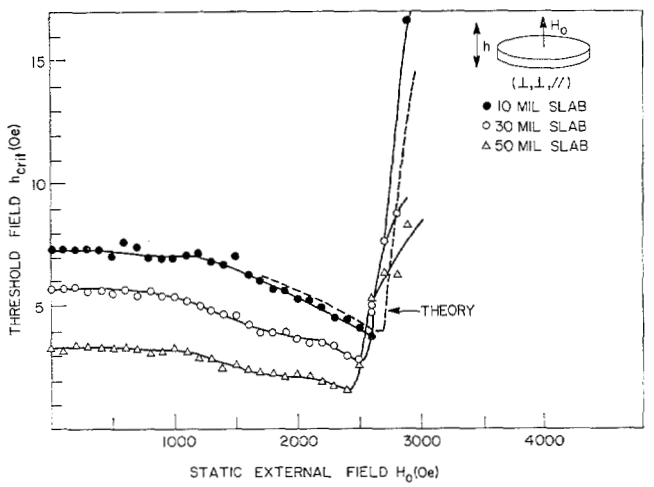

Fig. 2. Threshold field h_{crit} as a function of static external field H_0 for ($\perp,\perp,\parallel$) configuration. Data for 10-, 30-, and 50-mil-thick disks are shown.

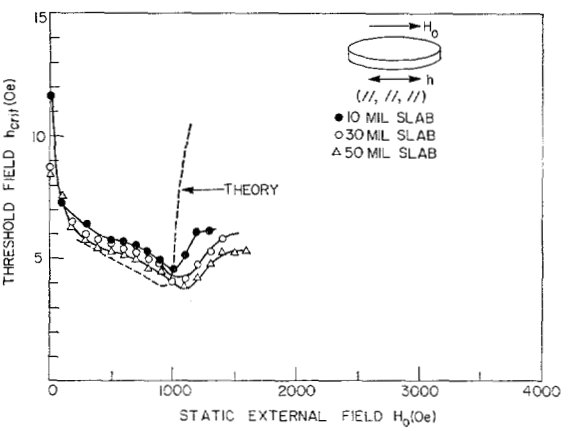

Fig. 3. Threshold field h_{crit} as a function of static external field H_0 for ($\parallel,\parallel,\parallel$) configuration. Data for 10-, 30-, and 50-mil-thick disks are shown.

as three Oe for the disk. The large change in h_{crit} for the disk suggests that the phenomenon is associated with surface damage inflicted during grinding or polishing and is greatest for samples with a large surface area to volume ratio. It should be noticed that the sign of the change upon annealing is not the same for the rod and disk. This characteristic may be associated with the specific nature of the surface strain interaction with the magnetization. The rod, the static field and magnetization are parallel to the surface, while for the disk, they are normal to the sample surface.

B. Parallel and Perpendicular Pumping in Thin Disks

Additional data were obtained for parallel and perpendicular pumping as a function of disk thickness, static field direction, and pump direction. The results are shown in Figs. 2–6. The threshold h_{crit} is displayed as a function of static field H_0 with the disk thickness as a parameter. The field configurations are indicated in the upper right-hand corner of each figure. The data were obtained on 1-cm-diameter polycrystalline YIG disks. To simplify the discussion each configuration is labeled by three indices, such as ($\perp,\perp,\parallel$) for Fig. 2, to indicate the static field and microwave field orientations with respect to the disk plane and the microwave field direction with respect to the static field.

The general characteristics of the results shown in Figs. 2 to 6 are summarized in Table I. The following generalizations can be made: 1) the thickness dependence is significant only when the microwave field is directed normal to the plane of the disk; 2) the minimum h_{crit} position is generally larger for normally magnetized disks than for in-plane magnetized disks; 3) the increase in h_{crit} at high field is sharp only for the normally magnetized disks; 4) large changes in h_{crit} upon demagnetization occur only for disks initially saturated parallel to the disk plane.

In comparing any of the above results with theoretical considerations, dielectric effects in the microwave cavity must be taken into account. In the two configurations for which the data exhibit a large thickness dependence, the ($\perp,\perp,\parallel$) and ($\parallel,\perp,\perp$) configurations, the disks are positioned in the TE_{102} microwave cavity with the microwave field normal to the disk plane. For these two configurations, portions of the sample are in a region of strong electric field directed parallel to the disk plane, and it is expected that dielectric loading might significantly influence the microwave field calibration in terms of the incident power for the cavity. In order to check this possibility, data

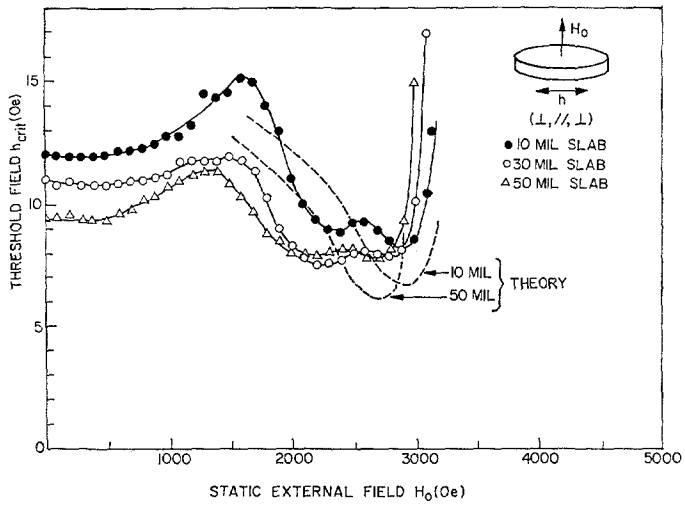

Fig. 4. Threshold field h_{crit} as a function of static external field H_0 for (⊥,||,⊥) configuration. Data for 10-, 30-, and 50-mil-thick disks are shown.

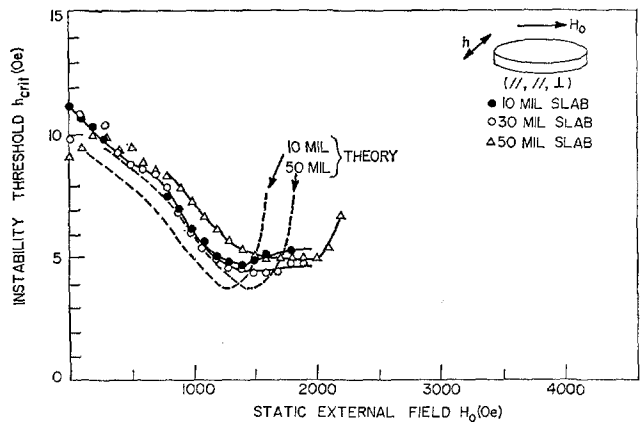

Fig. 5. Threshold field h_{crit} as a function of static external field H_0 for (||,||,⊥) configuration. Data for 10-, 30-, and 50-mil-thick disks are shown.

were obtained for all the configurations with a 10-mil YIG disk in contact with dielectric disks. It was found that thick dielectric disks had the same effect in reducing the apparent h_{crit} for the (⊥,⊥,||) and (||,⊥,⊥) configurations that thick magnetic disks did. For the (||,||,||) and (||,||,⊥) configurations, where the electric field is essentially zero over the sample, the dielectric disks had no effect on the results. For the (⊥,||,⊥) configuration, where the electric field is normal to the disk plane, a small decrease was noted for thick dielectric slabs. Dielectric loading of the cavity by the large disk samples appears to be responsible for most of apparent h_{crit} thickness dependence for the (⊥,⊥,||) and (||,⊥,⊥) configurations.

Theoretical curves for comparison with the data were calculated according to the procedure described in Section III-A and are shown as dashed lines in Figs. 2–6. Parallel pump curves were calculated using ΔH_k values determined from parallel pump data on spheres (see Appendix). Consider the comparison for the two parallel pumping configurations, (⊥,⊥,||) and (||,||,||), in Figs. 2 and 3. In each figure only one theoretical curve is plotted. For parallel pumping, the coupling which leads to instability is directly between the microwave pump field and the spin wave which goes unstable. This coupling is independent of disk thickness. Therefore h_{crit} is not expected to be thickness dependent, except for a small shift because of the change in the static demagnetizing field with the thickness. For the (⊥,⊥,||) configuration and the data in Fig. 2, the observed thickness dependence is due to dielectric effects as discussed above, since the microwave field is normal to the disk. For the thinnest disk, where such effects are less important, the agreement is quite good. For the other parallel pump configuration (||,||,||), the theoretical curve is the same as in Fig. 2, except it is shifted to lower field by $4\pi M$ due to the decrease in the internal demagnetizing field. At fields below the minimum h_{crit} position H_0^{min}, the theoretical curve agrees quite well with the data. Above this minimum, however, the experimental h_{crit} does not increase as rapidly as the theoretical curve. The slow rise in h_{crit} for $H_0 > H_0^{min}$ is a common feature of the threshold for all the in-plane magnetized disk configurations. It is probably due to the nonuniform demagnetizing field which is larger near the edges of the disk than in the center.

Now consider the results for perpendicular pumping, summarized in Figs. 4–6. Theoretical curves are indicated by dotted lines. For perpendicular pumping, h_{crit} depends on the uniform precession amplitude, which is influenced by sample shape. The threshold should exhibit a dependence on disk thickness which is related to the efficiency with which the microwave field excites the uniform precession. For the (⊥,||,⊥) configuration and the data in Fig. 4, (1) applies. As the disk thickness increases, $|\alpha_0|$ increases and the threshold decreases. The two theoretical curves in Fig. 4 express the above considerations quantitatively. The magnitude of the decrease in the theoretical h_{crit} (for $H_0 < H_0^{min}$) is in agreement with the data. The general shape of the curves were discussed in Section III-A. The shift of the h_{crit} minimum to lower static field is due to the reduction in the static internal field as the thickness increases and N_z decreases.

In order to discuss the remaining two perpendicular pump cases, it is necessary to consider the form of α_0 when the sample does not have rotational symmetry about the H_0 direction. If the static field and microwave field are along two principal axes of an ellipsoidal sample characterized by demagnetizing factors N_z and N_x, respectively, the uniform precession amplitude is given by (1) with $\omega_0 - \omega$ replaced by $(XY - \omega^2)/(\omega + Y)$, where

$$X = \gamma[H_0 + (N_x - N_z)4\pi M] \tag{3a}$$

$$Y = \gamma[H_0 + (N_y - N_z)4\pi M]. \tag{3b}$$

In (3), N_y is the demagnetizing factor along the remaining principal axis.

The data in Fig. 5 for the (||,||,⊥) configuration (H_0 and h_0 both parallel to the disk plane) indicate that for

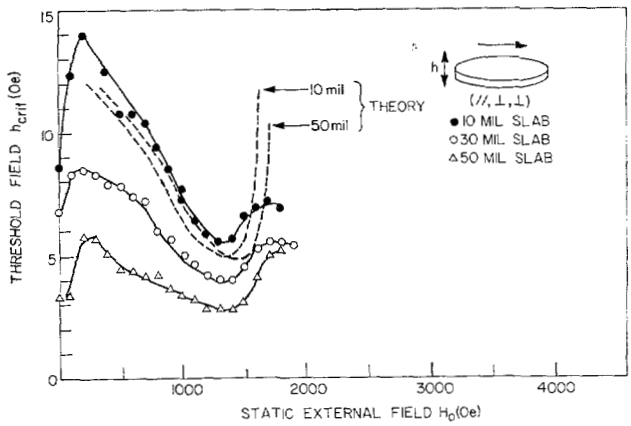

Fig. 6. Threshold field h_{crit} as a function of static external field H_0 for (||,⊥,⊥) configuration. Data for 10-, 30-, and 50-mil-thick disks are shown.

this configuration, h_{crit} is an increasing function of thickness for $H_0 < H_0^{min}$. The theoretical h_{crit} also increases with thickness. For this configuration, the y direction is normal to the disk and, consequently, N_y, Y, and $|\alpha_0|$ decrease with increasing thickness, so that h_{crit} is expected to increase. As mentioned above, the increase in h_{crit} at static fields above the minimum for in-plane magnetized disks is not as rapid as expected theoretically. Below the minimum, however, the agreement between the theory and the data is quite good. Finally, consider the results for the (||,⊥,⊥) configuration shown in Fig. 6 where H_0 is parallel to the disk plane and h_0 is normal to the disk. For this configuration, the data for the 10-mil slab are in good agreement with the theory except for the slow increase for $H_0 > H_0^{min}$. The data, however, exhibit a strong decrease in h_{crit} with increasing thickness which is related to dielectric loading since h_0 is normal to the disk plane. No strong dependence is expected theoretically. The y direction is in the plane of the disk (normal to H_0 and h) and H_0 is also in the disk plane. N_y and N_z are equal and $\omega + Y = \omega + \gamma H_0$ is independent of thickness.

C. Thresholds for Partially Magnetized Samples

The above discussion has been concerned with the results for saturated systems. It has been shown that threshold field data for a large variety of situations can be explained on the basis of spin-wave instability theory. In order to apply any of these results to partially magnetized systems, however, it is necessary to establish a connection between domain structure and the threshold fields. Such a connection is the subject of the remainder of this section. In the absence of any quantitative description of the domain structure, the treatment will be primarily qualitative. Domain structure considerations have previously been invoked [5] to qualitatively account for the dependence of h_{crit} on the pump angle between h and H_0 for partially magnetized spherical samples. Domain structure considerations may also be invoked to account for the threshold field behavior below saturation for the thin-disk data summarized in Figs. 2–6. First consider the results in Fig. 2 for parallel pumping with H_0 normal to the plane of the disk, the (⊥,⊥,||) configuration. The disk begins to demagnetize for $H_0 \approx 4\pi M$ or approximately 1750 Oe. At higher fields the magnetization is oriented normal to the disk and parallel to the microwave field by the static field H_0. For $H_0 \leq 1750$ Oe, the internal field is essentially zero and domains form as demagnetization processes act to minimize the free energy of the sample. As is evident from Fig. 2, h_{crit} for the (⊥,⊥,||) configuration does not exhibit any sharp changes during demagnetization, but increases gradually to approximately 7 Oe at $H_0 = 0$ (for the 10-mil disk), generally following the curve for the data above saturation. This smooth dependence indicates that the magnetization direction with respect to the microwave field polarization direction does not undergo any major reorientation upon demagnetization. It may be concluded, therefore, that in the partially magnetized or demagnetized material the domains are aligned in directions which are approximately parallel to the disk normal. Admittedly, this model is a gross oversimplification for polycrystalline YIG material which is cut into thin disks by mechanical means, and which clearly has considerable surface damage and interior defects. Nevertheless, such a model provides an approximate working basis for a consistent interpretation of the results.

This simple domain model also provides a consistent explanation of the results for the other configurations. For the domain structure suggested above, configurations (||,||,||), (⊥,||,⊥), and (||,||,⊥) are all equivalent at $H_0 = 0$. Only the orientation of h with respect to the disk is important. As shown by the data in Figs. 3–5 the values of h_{crit} at $H_0 = 0$ for these configurations are all comparable. For the (||,||,||) configuration (Fig. 3), demagnetization causes a change from parallel to perpendicular pumping, so that the h_{crit} field dependence changes abruptly below saturation. For the (⊥,||,⊥) configuration (Fig. 4), the abrupt change in h_{crit} comes from the change in shape of the single domain regions. Above saturation, $N_z \approx 1$ and $N_t \approx 0$ are satisfied. At $H_0 = 0$, the domain model suggests that $N_z \approx 0$ and $N_t \approx 1/2$ are more appropriate. For the (||,||,⊥) configuration (Fig. 5), $N_z \approx 0$ is satisfied both above saturation and at $H_0 = 0$. There is no abrupt change in h_{crit} below saturation. For the remaining configuration (||,⊥,⊥) in Fig. 6, demagnetization causes a change from perpendicular to parallel pumping. Consequently, h_{crit} changes abruptly as the sample demagnetizes. At $H_0 = 0$ the (||,⊥,⊥) configuration and the (⊥,⊥,||) configuration (Fig. 2) are equivalent and the threshold values are comparable.

Conclusion

This investigation has accomplished two objectives. 1) The effect of sample shape and pump configuration on the threshold for saturated systems has been characterized and compared with theory. 2) Data for partially magnetized disks have been obtained which can be explained on the basis of qualitative domain structure considerations.

The experimental data were obtained by using a semi-automated instrumentation system which enables h_{crit} determinations to be made accurately and quickly. Perpendicular pump data for axially magnetized rods, spheres, and normally magnetized slabs indicate that gross changes in sample shape have a large influence on h_{crit} and that annealing also changes h_{crit} for samples with large surface-area-to-volume ratios. Apart from modifications due to annealing and demagnetizing field effects, the data are consistent with theory. Parallel and perpendicular pump data for disk-shaped samples have been obtained which are also consistent with theory. For configurations with the microwave field normal to the disk, dielectric effects in the microwave cavity must be taken into account.

The results for partially magnetized disk samples indicate that the theory is applicable to these multidomain systems, if domain shape is taken into account. The disk data can be explained if a domain structure consisting of rod-shaped domains normal to the disk plane is assumed. Although such a domain model represents a gross over-simplification of the demagnetization processes involved, it appears to be qualitatively correct. The consistent correlations between the data and the theory provide convincing evidence that domain shape plays essentially the same role in determining the threshold for partially magnetized samples that sample shape does for saturated materials.

Appendix

As mentioned briefly in Section III, ΔH_k determinations from data on spherical samples were used to obtain theoretical curves of the threshold h_{crit} as a function of static field for the other sample shapes. The $\Delta H_k(\boldsymbol{k})$ from parallel pump data were used to calculate the parallel pump curves. The $\Delta H_k(\boldsymbol{k})$ from perpendicular pump data were used to obtain the perpendicular pump curves. The parallel pump ΔH_k increased from about 2.0 Oe at low k to 3.4 Oe at $k = 5 \times 10^5$ cm^{-1}. The perpendicular pump ΔH_k increased from 2.7 Oe at low k to 3.4 Oe at 5×10^5 cm^{-1}. These values of ΔH_k versus k for the two pump configurations are nearly the same. The ΔH_k appears to exhibit no strong dependence on the spin-wave angle θ_k between $\boldsymbol{k}$ and $\boldsymbol{M}$ for $k \neq 0$ ($\theta_k \approx \pi/4$ for perpendicular pumping and $\theta_k = \pi/2$ for parallel pumping). Consequently, those portions of the theoretical curves for $H_0 < H_0^{\min}$ are relatively independent of the configuration used to determine ΔH_k. This result is important because most of the conclusions of the present study are based on these low field portions of the butterfly curves.

The ΔH_k results indicate that significant discrepancies exist for $k \approx 0$, as shown by the values of 2.7 and 2.0 Oe cited above and by the observed dependencies of ΔH_k on θ_k. At $k \approx 0$, the parallel pump ΔH_k increases from 2.0 Oe at $\theta_k = \pi/2$ to a maximum of 4.2 Oe near $\theta_k = \pi/4$ and then decreases slowly. The perpendicular pump ΔH_k increases from 2.7 Oe at $\theta_k \approx \pi/4$ to 5 Oe at $\theta_k = 20°$, the limit of the present data. These differences affect only the portions of the theoretical curves for $H_0 > H_0^{\min}$. The theoretical results in this region can only be considered as approximate. Although this paper is not concerned with the spin-wave linewidth as such, two points which may have a bearing on the above results should be pointed out. 1) Application of the theory to calculate butterfly curves involves a minimization procedure to determine the particular $\boldsymbol{k}$ with the lowest threshold. This minimization should include the $\boldsymbol{k}$ dependence of ΔH_k. In order to extract ΔH_k from the analysis it was necessary to neglect the k dependence in the minimization. The strong θ_k dependences suggested by the results indicate that such a procedure is subject to error, particularly for perpendicular pumping. 2) The spin-wave theory is not strictly valid for $k \approx 0$. It is necessary to take proper account of the boundary conditions at the surface of the sample. The angular dependence of ΔH_k should prove to be an interesting subject for future investigation.

Acknowledgment

The authors wish to thankfully acknowledge E. Schlömann for many helpful discussions concerning spin-wave instability theory and the present experimental results, and J. Hillier for his careful and diligent attention to the microwave measurements.

References

[1] C. E. Patton, "Theory for the first-order spin-wave instability threshold in ferromagnetic insulators of ellipsoidal shape with an arbitrary pumping configuration," *J. Appl. Phys.*, vol. 40, pp. 2837–2843, June 1969.
[2] H. Suhl, "The theory of ferromagnetic resonance at high signal powers," *J. Phys. Chem. Solids*, vol. 1, pp. 209–227, 1957.
[3] E. Schlömann, J. J. Green, and U. Milano, "Recent developments in ferromagnetic resonance at high power levels," *J. Appl. Phys.*, vol. 31, pp. 386S–395S, May 1960.
[4] J. J. Green and T. Kohane, "Testing of ferrite materials for microwave applications," *SCP and Solid State Tech.*, vol. 7, pp. 46–54, August 1964.
[5] J. J. Green, E. Stern, and C. E. Patton, "Threshold microwave field amplitude for the unstable growth of spin waves under oblique pumping," *J. Appl. Phys.*, vol. 40, pp. 172–177, January 1969.